The Japanese Guidelines for the treatment of chronic hepatitis C recommend low-dose interferon monotherapy when the ALT level is controllable by the treatment [10]. Shiffman et al. [4] reported that a reduction in the HCV-RNA titer could be used to predict which patients would achieve a histological response and could be potential candidates for maintenance interferon therapy. In the present case, however, although there was no decrease in the ALT level or HCV-RNA titer, liver function improved gradually as a result of the IFN-β maintenance therapy. To access the justification of continuation of IFN therapy, we have adopted ^{99m}Tc-GSA SPECT analysis that can readily be performed and allows evaluation of hepatic functional reserve and the degree of hepatic inflammation and fibrosis. Improvement of the data obtained by ^{99m}Tc-GSA SPECT analysis justified continuation of the treatment. ^{99m}Tc-GSA SPECT analysis is clinically useful for patients with this condition.

IFN-α and -β are both used for the treatment of chronic hepatitis C. Both recognize common interferon receptors, and express IFN activity. IFN-α and -β are well known to have an anti-fibrotic effect in damaged liver [9, 11]. IFN-β has higher affinity for the IFN receptor than IFN-α and consequently shows stronger induction of IFN-regulated genes [12]. One explanatory hypothesis for the anti-fibrotic effect is that IFN-β strongly reduces the expression of mRNAs for transforming growth factor-β, basic fibroblast growth factor, collagen type I A2 and tissue inhibitor of metalloproteinase I, which are related to the progression of liver fibrosis [9]. Another plausible hypothesis may be that IFN-β enhances the expression of interleukin 10 [13], which had been reported to decrease disease activity in chronic hepatitis C patients [14]. We thus considered that IFN-β might be beneficial for some patients who were resistant to IFN-α.

In conclusion, the present case was considered to offer important information that ^{99m}Tc-GSA SPECT analysis was helpful in justifying continuation of IFN therapy for IFN-non-responsive chronic hepatitis C without frequent liver biopsy.

References

1. Ikeda K, Saitoh S, Suzuki Y, Kobayashi M, Tsubota A, Koida I, et al. Disease progression and hepatocellular carcinogenesis in patients with chronic viral hepatitis: a prospective observation of 2215 patients. J Hepatol. 1998;28:930–8.
2. Hoofnagle JH, di Bisceglie AM. The treatment of chronic viral hepatitis. N Engl J Med. 1997;336:347–56.
3. Ghany MG, Strader DB, Thomas DL, Seeff LB. Diagnosis, management, and treatment of hepatitis C: an update. Hepatology. 2009;49:1335–74.
4. Shiffman ML, Hofmann CM, Contos MJ, Luketic VA, Sanyal AJ, Sterling RK, et al. A randomized, controlled trial of maintenance inteferon therapy for patients with chronic hepatitis C virus and persistent viremia. Gastroenterology. 1999;117:1164–72.
5. Nomura H, Kashiwagi Y, Hirano R, Tanimoto H, Tsutsumi N, Higashi M, et al. Efficacy of low dose long-term interferon monotherapy in aged patients with chronic hepatitis C genotype 1 and its relation to alpha-fetoprotein: a pilot study. Hepatol Res. 2007;37:490–7.
6. Akuta N, Suzuki F, Kawamura Y, Yatsuji H, Sezaki H, Suzuki Y, et al. Efficacy of low-dose intermittent interferon-alpha monotherapy in patients infected with hepatitis C virus genotype 1b who were predicted or failed to respond to pegylated interferon plus ribavirin combination therapy. J Med Virol. 2008;80:1363–9.
7. Di Bisceglie AM, Shiffman ML, Everson GT, Lindsay KL, Everhart JE, Wright EC, et al. Prolonged therapy of advanced chronic hepatitis C with low-dose peginterferon. New Engl J Med. 2008;359:2429–41.
8. Sugahara K, Togashi H, Takahashi K, Onodera Y, Sanjo M, Misawa K, et al. Separate analysis of asialoglycoprotein receptors in the right and left hepatic lobes using Tc-99m-GSA SPECT. Hepatology. 2003;38:1401–9.
9. Tanabe J, Izawa A, Takemi N, Miyauchi Y, Torii Y, Tsuchiyama H, et al. Interferon-beta reduces the mouse liver fibrosis induced by repeated administration of concanavalin A via the direct and indirect effects. Immunology. 2007;122:562–70.
10. Kumada H, Okanoue T, Onji M, Moriwaki H, Izumi N, Tanaka E, et al. Guidelines for the treatment of chronic hepatitis and cirrhosis due to hepatitis C virus infection for the fiscal year 2008 in Japan. Hepatol Res. 2010;40:8–13.
11. Yagura M, Murai S, Kojima H, Tokita H, Kamitsukasa H, Harada H. Changes of liver fibrosis in chronic hepatitis C patients with no response to interferon-alpha therapy: including quantitative assessment by a morphometric method. J Gastroenterol. 2000;35:105–11.
12. Murata M, Nabeshima S, Kikuchi K, Yamaji K, Furusyo N, Hayashi J. A comparison of the antitumor effects of interferon-alpha and beta on human hepatocellular carcinoma cell lines. Cytokine. 2006;33:121–8.
13. Izuma M, Kobayashi K, Shiina M, Ueno Y, Ishii M, Shimosegawa T, et al. In vitro cytokine production of peripheral blood mononuclear cells in response to HCV core antigen stimulation during interferon-beta treatment and its relevance to sCD8 and sCD30. Hepatol Res. 2000;18:218–29.
14. Nelson DR, Tu Z, Soldevila-Pico C, Abdelmalek M, Zhu H, Xu Y, et al. Long-term interleukin 10 therapy in chronic hepatitis C patients has a proviral and anti-inflammatory effect. Hepatology. 2003;38:859–68.

Clin J Gastroenterol (2011) 4:273–277
DOI 10.1007/s12328-011-0237-6

CASE REPORT

A case of monocular blindness as the initial presentation of hepatocellular carcinoma with skull metastasis

Junitsu Ito · Takafumi Saito · Akiko Iwaba · Yoshihiro Suzuki · Mai Sanjo · Rika Ishii · Chikako Sato · Hiroaki Haga · Kazuo Okumoto · Yuko Nishise · Hisayoshi Watanabe · Koji Saito · Hitoshi Togashi · Sumio Kawata

Received: 18 January 2011 / Accepted: 14 June 2011 / Published online: 15 July 2011

Abstract A 52-year-old man suffering from monocular blindness, with light perception only, was admitted to our hospital. The symptom had begun as low vision and developed rapidly within 3 weeks into monocular blindness in the right eye, with no other systemic manifestations. Imaging examinations revealed multiple hepatocellular carcinomas in the cirrhotic liver, and tumors at the skull base and vertebra. A pathological and immunochemical study of specimens obtained by endoscopic transnasal tumor biopsy and laminectomy revealed them to be metastatic hepatocellular carcinomas (HCCs). Although the patient underwent radiation therapy and chemotherapy, he died 5 months after admission to our hospital. The cranial HCC, involving only the optic canal, may have disturbed the optic nerve in preference to the other cranial nerves. This is the first report of a HCC patient with monocular blindness as the initial presentation of the disease.

J. Ito (✉) · T. Saito · M. Sanjo · R. Ishii · C. Sato · H. Haga · K. Okumoto · Y. Nishise · H. Watanabe · K. Saito · S. Kawata
Department of Gastroenterology, Yamagata University Faculty of Medicine, 2-2-2 Iida-Nishi, Yamagata 990-9585, Japan
e-mail: jxi9@med.id.yamagata-u.ac.jp

A. Iwaba
Department of Diagnostic Pathology, Yamagata University Faculty of Medicine, 2-2-2 Iida-Nishi, Yamagata 990-9585, Japan

Y. Suzuki
Department of Gastroenterology, Nihonkai General Hospital, 30 Akiho-cho, Sakata, Yamagata 998-8501, Japan

H. Togashi
Health Administrative Center, Yamagata University, 1-4-12 Kojirakawa, Yamagata 990-9560, Japan

Keywords Blindness · Hepatocellular carcinoma · Metastasis

Introduction

Hepatocellular carcinoma (HCC), one of the most common types of cancer worldwide, is characterized by poor presentation of specific symptoms until advanced stages. The incidence of HCC metastases has been reported from <5 to 36.7% in clinical records [1–3] and more frequently in autopsy cases [4]. Bone is the third most frequent site for HCC metastasis followed by the lung and the abdominal lymph nodes. The common bone metastatic sites are the vertebra, the rib, and the long bone; however, bone metastasis of HCC to the skull is very rare. The frequent presentations of bone metastatic HCC are an occasional painful sensation, headache, weakness of limbs, seizures, and symptoms associated with a disturbance of the cranial nerves [3].

To the best of our knowledge, this is the first report of a HCC patient with monocular blindness as the initial presentation of the disease.

Case report

A 52-year-old man suffering from monocular blindness, with light perception only, was admitted to our hospital in April 2009. The symptom had begun as low vision and developed rapidly within 3 weeks into monocular blindness in the right eye, with no other systemic manifestations. The patient consumed excessive alcohol for over 30 years. He also had a medical history of blood transfusion for

Table 1 Laboratory data on admission

Hematology		*Serology test*	
White blood cells	5960/μl	HBs-antigen	Negative
Hemoglobin	14.9 mg/dl	HBs-antibody	Negative
Platelets	176 × 10^3/μl	HBc-antibody	Positive
		HBV-DNA PCR	2.1 log/ml
Blood chemistry		HCV-antibody	Negative
Total bilirubin	0.9 mg/dl		
Direct bilirubin	0.3 mg/dl	*Tumor markers*	
AST	68 U/l	AFP	1881 ng/ml
ALT	38 U/l	PIVKA-II	6911 mAU/ml
Alkaline phosphatase	581 U/l	CEA	2.22 ng/ml
γ-GTP	198 U/l	CA19-9	13.2 U/ml
Total protein	7.4 g/dl		
Albumin	3.9 g/dl	*Others*	
		ICG(15)	29%
Coagulation			
PT%	101%		

AST aspartate aminotransferase, *ALT* alanine aminotransferase, *γ-GTP* glutamyltransferase, *HBs* hepatitis B virus surface, *HBc* hepatitis B virus core antigen, *PCR* polymerase chain reaction, *AFP* α-fetoprotein, *PIVKA-II* protein induced by vitamin K absence, *CEA* carcinoembryonic, *CA19-9* carbohydrate antigen 19-9, *ICG(15)* indocyanine green 15 min retention rate

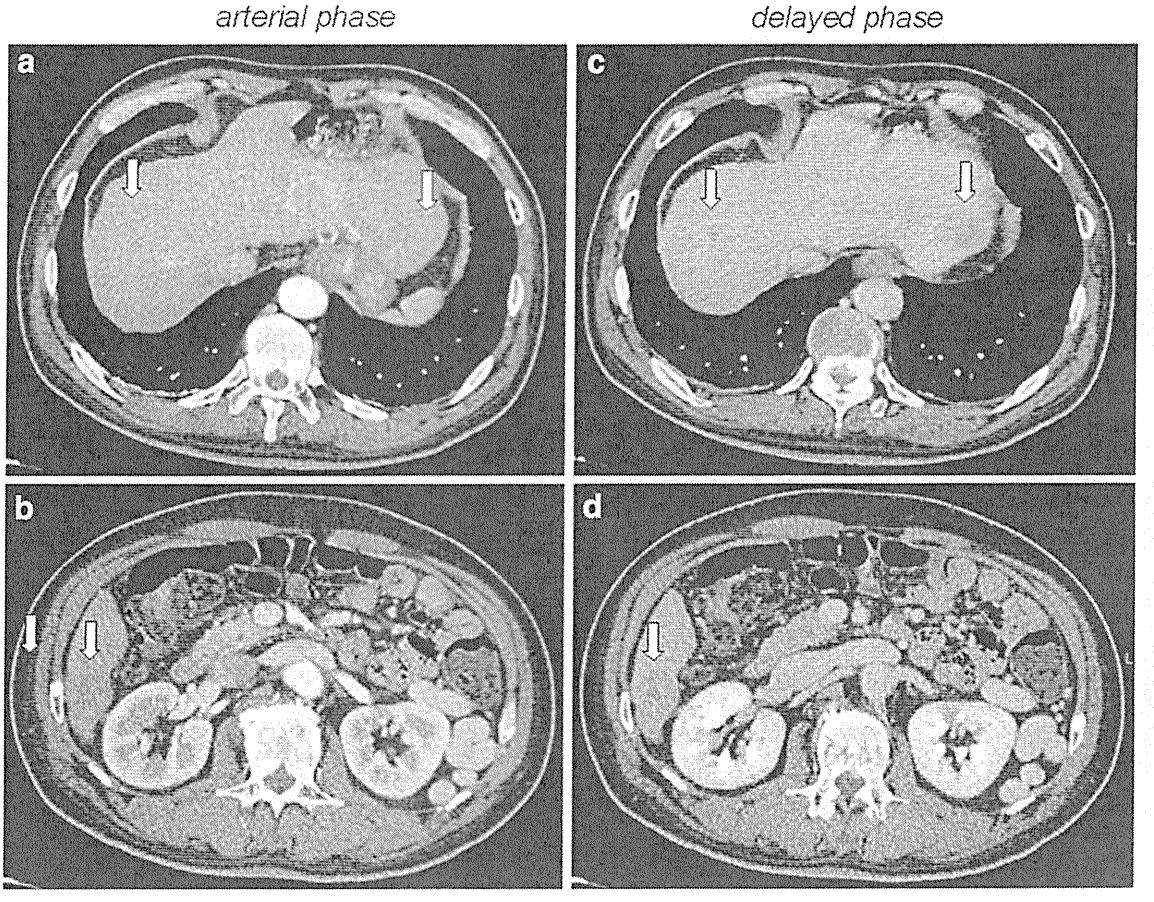

Fig. 1 Abdominal computed tomography scan on admission. *Arrows* indicate the mass in each scan

hemorrhagic gastric ulcer in 1990 and mitral valve plasty for mitral regurgitation in 2007.

Laboratory investigation on admission revealed negative for serum hepatitis B surface antigen; however, serum hepatitis B virus DNA (HBV-DNA) was substantively positive by polymerase chain reaction (PCR). Thus the liver dysfunction of this patient might be due not only to alcohol abuse but also to 'occult hepatitis B' infection.

Other laboratory findings were: total bilirubin 0.9 mg/dl (normal 0.2–1.3); serum aspartate aminotransferase 68 U/l (normal 13–33); alanine aminotransferase 38 U/l (normal 8–42); indocyanine green (ICG) 15 min retention rate 29.0% (normal 0–10). While serum levels of carcinoembryonic antigen (CEA), carbohydrate antigen 19-9 (CA 19-9) were within normal range, tumor markers for HCC were elevated: α-fetoprotein (AFP) 1881 ng/ml (normal 0–6.2); protein induced by vitamin K absence (PIVKA-II) 6911 mAU/ml (normal 0–40) (Table 1). Enhanced computed tomography (CT) showed the 32 × 22 mm, 36 × 24 mm and 9 × 9 mm lesions, all of which were barely enhanced in the arterial phase study (Fig. 1a, b) and hypoenhanced in the portovenous study (Fig. 1c, d) in segments 2, 6 and 8 of the cirrhotic liver, respectively. Cranial magnetic resonance imaging (MRI) showed a tumor involving the optic canal spread across the right sphenoid sinus and sella turcica. It also showed the tumor to have slight high intensity on T1-weighted and low intensity on T2-weighted images. The tumor was enhanced homogeneously (Fig. 2a). Spinal MRI showed spinal tumors at cervical vertebrae (C1, C2), thoracic vertebrae (Th5, Th6) and sacrum (S1 and S2). The tumors of the thoracic vertebrae, in particular, seemed to press against the spinal cord intensively (Fig. 2b).

An endoscopic transnasal tumor biopsy was performed [5]. A microscopic examination of the specimen showed that the tumor was mainly composed of palisaded cells with yellow pigment-like bile (Fig. 3). After the patient was admitted to our hospital, leg paralysis emerged and developed rapidly. Therefore, emergency laminectomy with posterior fixation was performed [6]. Microscopic examination of the thoratic tumor specimen also showed palisaded tumor cells. The immunochemical expression of HepPar1 and cytokeratin (CK) 8 were positive [7–9] (Fig. 3). Taken together, both tumors were diagnosed as metastasis of moderately differentiated HCC.

The patient underwent radiation therapy: 3 Gy × 12 times for skull, 3 Gy × 12 times for cervical vertebrae, 3 Gy × 15 times for thoracic vertebrae; 3 Gy × 15 times for sacrum. He then underwent continuous infusion of 5-fluorouracil (750 mg on days 1–5), mitoxantrone (10 mg

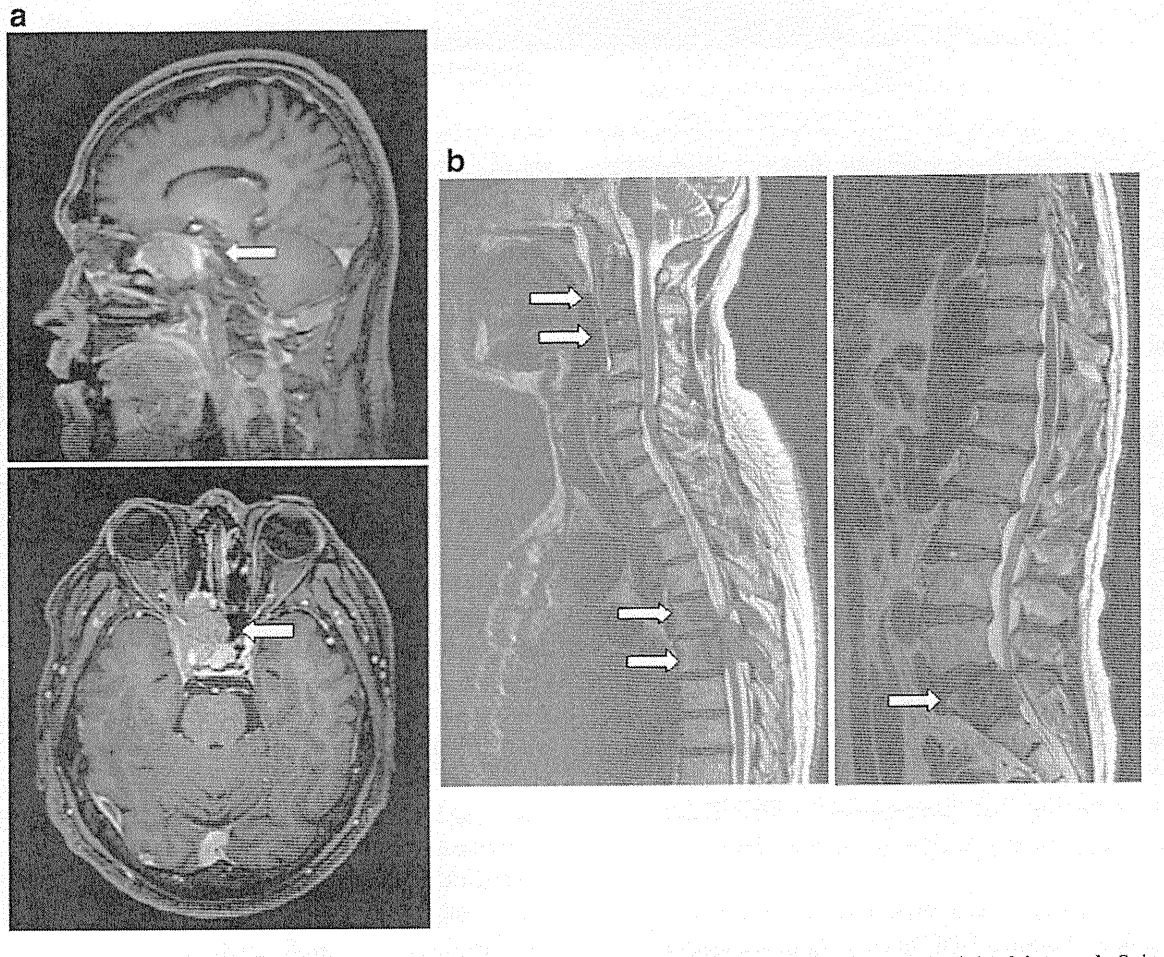

Fig. 2 Cranial and spinal magnetic resonance imaging (*MRI*) on admission. **a** Enhanced cranial MRI, T1-weighted image. **b** Spinal MRI, T2-weighted image. *Arrows* indicate the mass in each image

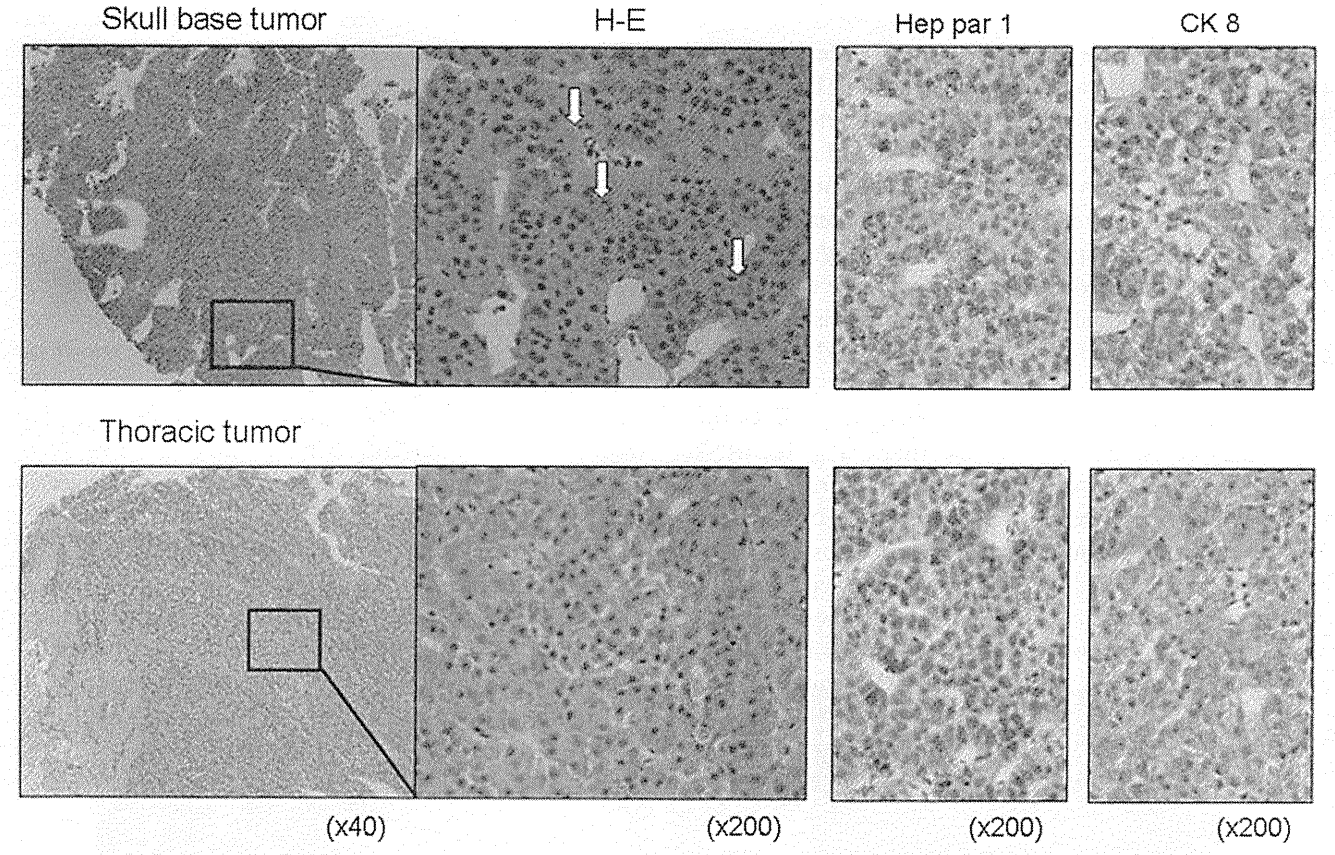

Fig. 3 Microscopic findings. *Upper panel* shows the specimen of the skull base tumor obtained by endoscopic transnasal tumor biopsy. *Lower panel* shows the specimen of the thoracic tumor obtained by laminectomy. Hematoxylin and eosin (H&E), HepPar1, and cytokeratin (CK) 8 antibodies were used for immunocytochemical study. *Arrows* indicate bile pigments

on day 1) and cisplation (100 mg on day 1) (FMP) therapy [10]. However, the general condition of the patient deteriorated and he died 5 months after admission to our hospital.

Discussion

HCC is known as a very aggressive cancer causing intrahepatic metastases via portal vein and hepatic veins at early stages, while distant metastases usually occur at late stages, possibly via hematogenous or lymphatic pathways [1]. Therefore, it is important to find the primary HCC in the liver at an early stage for a better prognosis for the patient. However, HCC is also known to be a cancer characterized by poor presentation of specific symptoms until advanced stages. Thus, the symptoms due to the metastasis sometimes become the first presentation of the disease and provide an opportunity to find the primary HCC, as in our case.

Some reports have described the most common clinical presentations of cranial HCC to be scalp mass, neurological deficits, headache and seizures [3, 11, 12]. Theoretically, the clinical symptoms should be associated with the cranial site of the tumor involved, i.e., scalp mass and headache are likely due to calvarial metastases, and cranial nerve deficits are likely due to skull base metastases. In this report, the skull base tumor of the patient located as involving only the optic canal may have disturbed the optic nerve in preference to the other cranial nerves. When we focus on the symptom of visual disturbance, the most common previously reported visual disturbances from HCC are homonymous hemianopia, diplopia, and proptosis, which are mostly due to orbit metastasis [13–16]. Blindness is a very rare symptom of metastatic tumors derived from the trunk of the body, like HCC, gastric cancer [17], and esophageal cancer [18]. By a Medline search via PubMed, HCC is reported in one case as presentating with an occipital haematoma after therapy for metastatic HCC [19]. To the best of our knowledge, blindness has not been reported as the initial presentation for metastatic HCC.

Hepatitis C virus (HCV) and HBV infection are well known major causes of HCC, however, the incidence of HCC is lower in alcoholic cirrhosis in the absence of HCV and HBV infection [20]. In this paper, the laboratory

investigation of the patient revealed negative hepatitis B surface antigen, however, HBV-DNA PCR was substantively positive. We examined HBV-DNA PCR three times and the results were all positive: 2.5, 2.5, and 2.1 log copy/ml. Occult HBV infection is defined as serologically undetectable hepatitis B surface antigen despite the presence of circulating HBV-DNA, suggesting maintaining a potential risk for HCC development [21]. Thus, the liver dysfunction of this patient might be due not only to alcohol abuse but also to 'occult hepatitis B' infection, and the synergistic effect of this combination might be the main cause of HCC.

A strict diagnosis of metastatic HCC is usually difficult by noninvasive examination, because CT and MR images of metastatic HCC vary a great deal in each case [3]. Even though the specific tumor markers for HCC of our patient were high (AFP 1881 ng/ml; PIVKA-II 6911 mAU/ml), a histological diagnosis was necessary for the identification of primary cancer. Thus, we performed an immunocytochemical study of the specimen obtained by endoscopic transnasal tumor biopsy and laminectomy (Fig. 3). The result of the immunochemical expression of the effective markers for HCC, HepPar1 and CK 8 antibodies, suggested that the metastatic tumors were derived from hepatocyte [7–9]; both tumors were strictly diagnosed as metastasis of moderately differentiated HCC.

In conclusion, although blindness is an exceedingly rare symptom of HCC, it is necessary to be aware of it. To the best of our knowledge, this is the first report of a HCC patient with monocular blindness as the initial presentation of the disease.

References

1. Katyl S, Oliver JH III, Peterson MS, Ferris JV, Carr BS, Baron RL. Extrahepatic metastases of hepatocellular carcinoma. Radiology. 2000;216:698–703.
2. Natsuizaka M, Omura T, Akaike T, Kuwata Y, Yamazaki K, Sato T, et al. Clinical features of hepatocellular carcinoma with extrahepatic metastases. J Gastroenterol Hepatol. 2005;20:1781–7.
3. Hsieh CT, Sun JM, Tsai WC, Tsai TH, Chiang YH, Liu MY. Skull metastasis from hepatocellular carcinoma. Acta Neurochir. 2007;149:185–90.
4. Nakashima T, Okuda K, Kojiro M, Jimi A, Yamaguchi R, Sakamoto K, et al. Pathology of hepatocellular carcinoma in Japan. 232 consecutive cases autopsied in ten years. Cancer. 1983;51:853–77.
5. Ong YK, Solares CA, Carrau RL, Snyderman CH. New development in transnasal endoscopic surgery for malignancies of the sinonasal tract and adjacent skull base. Curr Opin Otolaryngol Head Neck Surg. 2010;18:107–13.
6. Doval DC, Bhatia K, Vaid AK, Pavithran K, Sharma JB, Hazarika D, et al. Spinal cord compression secondary to bone metastases from hepatocellular carcinoma. World J Gastroenterol. 2006;12:5247–52.
7. Kawai M, Saegusa Y, Kemmochi S, Harada T, Shimamoto K, Shibutani M, et al. Cytokeratin 8/18 is a useful immunohistochemical marker for hepatocellular proliferative lesions in mice. J Vet Med Sci. 2010;72:263–9.
8. Onofre AS, Pomjanski N, Buckstegge B, Böcking A. Immunocytochemical diagnosis of hepatocellular carcinoma and identification of carcinomas of unknown primary metastatic to the liver on fine-needle aspiration cytologies. Cancer. 2007;111:259–68.
9. Siddiqui MT, Saboorian MH, Gokaslan ST, Ashfraq R. Diagnostic utility of the HepPar1 antibody to differentiate hepatocellular carcinoma from metastatic carcinoma in fine-needle aspiration samples. Cancer. 2002;96:49–52.
10. Ikeda M, Okusaka T, Ueno H, Takezako Y, Morizane C. A phase II trial of continuous infusion of 5-fluorouracil, mitoxantrone, and cisplatin for metastatic hepatocellular carcinoma. Cancer. 2005;103:756–62.
11. Shibukawa M, Inagawa T, Katoh Y, Tokuda Y, Ohbayashi N, Yoshioka Y. A case of cranial metastasis of hepatocellular carcinoma (in Japanese with English abstract). No To Shinkei. 1995;47:1087–91.
12. Murakami R, Korogi Y, Sakamoto Y, Takhashi M, Okuda T, Yasunaga T, et al. Skull metastasis from hepatocellular carcinoma. CT, MR and angiographic findings. Acta Radiol. 1995;36:597–602.
13. Hsu SY, Chang FL, Sheu MM, Tsai RK. Homonymous hemianopia caused by solitary skull metastasis of hepatocellular carcinoma. J Neuroophthalmol. 2008;28:51–4.
14. Hirunwiwatkul P, Tirakunwichcha S, Meesuaypong P, Shuangshoti S. Orbital metastasis of hepatocelluar carcinoma. J Neuroophthalmol. 2008;28:47–50.
15. Quick AM, Bloomston M, Kim EY, Hall NC, Mayr NA. Complete response to radiation therapy of orbital metastasis from hepatocellular carcinoma. World J Gastroenterol. 2009;15:6000–3.
16. Srinivasan R, Krishnanand G. Cytologic diagnosis of metastatic hepatocellular carcinoma presenting as an orbital mass. A case report. Acta Cytol. 2007;51:83–5.
17. Harmon DC, Mark EJ, Vonsattel JP. Case 10-1999—a 53-year-old man with acute renal failure, cortical blindness, and respiratory distress. N Engl J Med. 1999;340:1099–106.
18. Teare JP, Whitehead M, Rake MO, Coker RJ. Rapid onset of blindness due to meningeal carcinomatosis from an oesophageal adenocarcinoma. Postgrad Med J. 1991;67(792):909–11.
19. Cho DC, Yi HJ, Ko Y, Oh SJ, Lee SR, Paik SS. Recurrent metastatic hepatocellular carcinoma presenting as consecutive "mirror image" intracerebral haematomas. J Clin Neurosci. 2005;12:699–702.
20. Fattovich G, Stroffolini T, Zagni I, Donato F. Hepatocellular carcinoma in cirrhosis: incidence and risk factors. Gastroenterology. 2004;127:S35–50.
21. De Mitri MS, Cassini R, Bernardi M. Hepatitis B virus-related hepatocarcinogenesis: molecular oncogenic potential of clear or occult infections. Eur J Cancer. 2010;46:2178–86.

肝臓　52巻11号　753-755（2011）

＜短　報＞

B型肝炎ウイルスジェノタイプB型感染高浸淫地区における感染実態の変遷

渡辺　久剛[1)*]　斎藤　貴史[1)]　冨田　恭子[1)]　佐藤智佳子[1)]　石井　里佳[1)]
芳賀　弘明[1)]　奥本　和夫[1)]　西瀬　雄子[1)]　河田　純男[2)]

はじめに：わが国において，B型肝炎ウイルス（HBV）感染者のHBVジェノタイプは，全体の80%以上を占めるC型がmajor typeであるが，その分布には地域特性が知られている．以前我々は，全国多施設共同研究の一環として，当科で診療したHBs抗原陽性者についてジェノタイプ調査をretrospectiveに行ったが，ジェノタイプB型が34.6%を占めていた[1)]．

また，HBVジェノタイプA型感染によるB型急性肝炎は都市部においてその拡がりが顕著であるが[2)3)]，地方においても増加傾向にあるものと推測され，今後の感染拡大が予想される．また肝炎の遷延化も指摘されており[4)]，ユニバーサルワクチン導入の是非を議論する上でも，その感染実態を把握することは重要である．HBVジェノタイプB型高浸淫地域における，最近のB型急性肝炎のジェノタイプによる感染実態は明らかではない．そこで，過去20年間における，当科のHBs抗原陽性例のHBVジェノタイプ別感染の変遷，およびB型急性肝炎におけるHBVジェノタイプの感染実態の変遷を検討した．

対象および方法：1990年から2009年まで，当科で診療したHBs抗原陽性全例にあたる430例を解析対象とした．これらのHBVジェノタイプを測定し，1990年から1999年（284例），2000年から2009年（146例）の二群に分けて，各HBVジェノタイプ別の感染頻度の変遷を検討した．HBVジェノタイプは当該期間内に初回受診した際の凍結保存血清を用いてretrospectiveに解析した．また430例の中で血清学的にB型急性肝炎と診断された34例について同様の検討を行った．B型急性肝炎の診断は，1）血清HBs抗原陽性かつIgM-HBc抗体陽性であること，2）他の肝炎の原因が血清学的に否定されていること，3）急性の肝機能障害を認め，過去に肝機能障害の既往がないこと，とした．

結果：HBs抗原陽性430例におけるジェノタイプ別のHBV感染者の割合は，A型11例（2.6%），B型194例（45.0%），C型150例（34.9%），D型4例（1.0%），分類あるいは検出不能による不明71例（16.5%）であった．1999年以前では，A型6例（2.1%），B型128例（45.1%），C型100例（35.2%）であったのに対し，2000年以降では，A型5例（3.5%），B型66例（45.2%），C型50例（34.2%）であった．いずれの年代においても，HBs抗原陽性例全体におけるジェノタイプの感染実態には変化は見られなかった．

B型急性肝炎34例のジェノタイプ別のHBV感染者の割合は，1999年以前の群に比較し2000年以降の群ではジェノタイプB型の割合が有意に低下し（10/17；58.8% vs. 1/17；5.9%；$p=0.012$），ジェノタイプA型の割合は増加傾向であった（2/17；11.8% vs. 5/17；29.4%，Fig.）．

当科で経過観察されているHBVジェノタイプA型感染によるB型急性肝炎症例7例を示す（Table）．ジェノタイプはすべてAe型であった．感染経路は，患者本人からの問診によればいずれも異性間性行為が疑われ，同性愛者はいなかった．また推定される感染地域は，不明である症例3，6を除けばいずれも山形県内であった．症例1は他の6例と異なり，自覚症状がなく，職場検診で初めてALT値の上昇とHBs抗原陽性を指摘され，IgM-HBc抗体陽性であったことから，B型急性肝炎と診断された．ラミブジンが投与されたが改善せず，その後ラミブジン耐性ウイルスが出現し，アデフォビルの投与によりALT値とウイルス量の低下を見た．肝機能異常を検診で初めて指摘されてから約3カ月後のラミブジン投与前の肝生検では，既に慢性肝炎（F1/A1）の組織像を呈していた．他の6例は，来院時にいずれも急性肝炎に特徴的な症状とALT値の高値を伴い，その後HBs抗原の陰性化を確認している．

1）山形大学医学部消化器内科学
2）兵庫県立西宮病院
*Corresponding author: h-watanabe@med.id.yamagata-u.ac.jp
＜受付日2011年8月10日＞＜採択日2011年9月17日＞

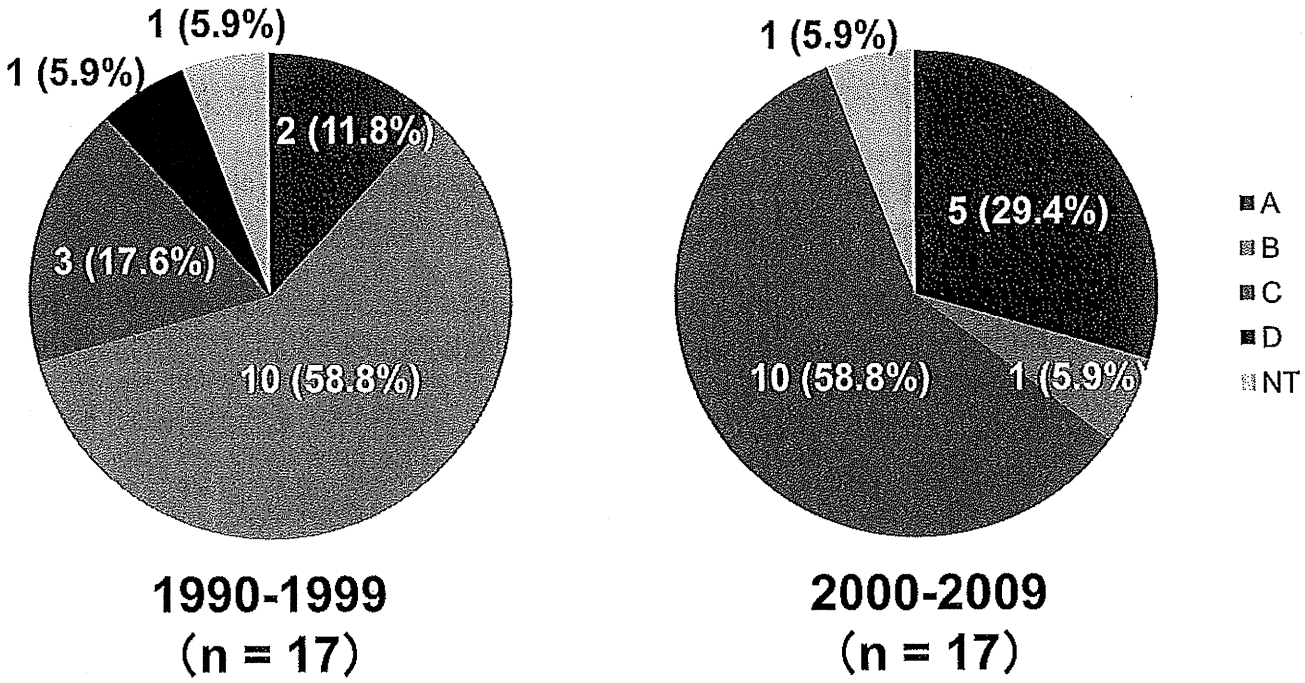

Fig. Distribution of HBV genotypes in acute hepatitis B
Genotype B was found in 58.8% between 1990 and 1999, 5.9% between 2000 and 2009, while the prevalence of genotype A was increased from 11.8% (1990-1999) to 29.4% (2000-2009).

Table Characteristics of 7 patients infected with genotype A

Case No.	Age (Years)	Sex	ALT* (IU)	IgM anti-HBc (S/CO)	HIV Ab	HBsAg clearance (months)	Outcome	Treatment	Route of Infection	Genotype
1	45	M	185	10.2	(−)	Persistently positive	chronicity	LAM	heterosexual	Ae
2	22	M	1282	41.3	(−)	4	resolved	ETV	heterosexual	Ae
3	26	M	2008	26.3	(−)	9	resolved	ETV	heterosexual	Ae
4	49	F	557	22.6	(−)	5	resolved	—	heterosexual	Ae
5	26	M	3650	29.9	(−)	3	resolved	—	heterosexual	Ae
6	56	M	2876	8.3	(−)	3	resolved	—	heterosexual	Ae
7	55	F	1414	7.2	(−)	5	resolved	—	heterosexual	Ae

LAM: Lamivudine, ETV: Entecavir
*the first medical examination on admission

考察：HBV ジェノタイプB型高浸淫地域において，HBs 抗原陽性例全体に占める HBV ジェノタイプを検討した結果，ジェノタイプB型およびC型の感染割合は過去と現在においてほとんど変化していないことが明らかとなった．

また過去 20 年における 34 例のB型急性肝炎の HBV ジェノタイプの検討では，1999 年以前にはジェノタイプB型感染者が半数を占めていたが，最近 10 年間ではわずかに 1/17 例とほとんど見られなくなっていた．従来 HBV ジェノタイプB型感染者が圧倒的に多い当施設において，ジェノタイプB型感染のB型急性肝炎例の割合が 2000 年以降に急激に低下していることは興味深い．一方，急性肝炎に占めるジェノタイプC型感染の割合はこの 10 年間で増加していたが，その理由としてジェノタイプA型感染の増加と相まって，本州における主なジェノタイプであるC型感染も地方へ広がって

きているためと推測する．

本研究では必ずしも一般の急性肝炎を反映しているとは言えないが，少なくとも過去にジェノタイプB型感染の頻度が高かった単一施設での観察では，ジェノタイプB型感染が減少し，ジェノタイプA型感染が確実に増加してきていることが明らかとなった．特に急性期に自覚症状を欠き検診などで偶然に見つかる例にも遭遇することから，地方におけるジェノタイプA型感染の拡大にも，今後は十分に留意する必要があるものと思われた．

結語：HBVジェノタイプB型感染の高浸淫地域において，この20年間で，HBs抗原陽性例全体に占めるジェノタイプB型感染の比率に変化はないものの，B型急性肝炎のジェノタイプの感染割合は，ジェノタイプB型が明らかに減少し，ジェノタイプA型が増加していた．肝炎の遷延化の問題も含め，全国的な疫学調査に基づいたB型肝炎対策が急務である．

本研究の一部は，厚生労働科学研究費補助金（肝炎等克服緊急対策研究事業）の助成を受けた．

索引用語：HBV genotype, acute hepatitis, genotype B

文献：1) Orito E, Ichida T, Sakugawa H, et al. Hepatology 2001; 34: 590—594　2) 山田典栄，四柳宏，小板橋優，他．肝臓　2008；49：553—559　3) Kobayashi M, Suzuki F, Arase Y, et al. J Gastroenterol 2004; 39: 844—850　4) Suzuki Y, Kobayashi M, Ikeda K, et al. J Med Virol 2005; 76: 33—39

英文要旨

Hepatitis B virus genotypes in a hyperendemic area for genotype B infection

Hisayoshi Watanabe[1]*, Takafumi Saito[1], Kyoko Tomita[1], Chikako Sato[1], Rika Ishii[1], Hiroaki Haga[1], Kazuo Okumoto[1], Yuko Nishise[1], Sumio Kawata[2]

To elucidate genotypes of HBV carriers in a hyperendemic area for HBV genotype B infection and to examine the changes over time in genotypes responsible for acute hepatitis B, 430 HBsAg-positive HBV carriers were determined by genotypes and compared the literal translation of infection status according to two time-period groups: a group seen between 1990 and 1999 and a group seen between 2000 and 2009.

In total, 45% had genotype B and 35% had genotype C in both time-period groups, indicating no changes in genotypes over time. Among 34 acute hepatitis B patients, the percentage of genotype B was significantly lower in the present group (5.9%) than in the past group (58.8%), while the prevalence of genotype A tended to have increased in the last 10 years.

In conclusion, there was an increase in acute hepatitis B infection by genotype A in a hyperendemic area for genotype B infection, even though there was no large change of genotypes between the present and the past percentages of subjects. A nation-wide surveillance of HBV infection status is a matter of urgency in terms of the universal vaccination for HBV.

Key words: HBV genotype, acute hepatitis, genotype B

Kanzo 2011; 52: 753—755

1) Department of Gastroenterology, Yamagata University School of Medicine, Yamagata, Japan
2) Hyogo Prefectural Nishinomiya Hospital, Nishinomiya, Japan
*Corresponding author: h-watanabe@medid.yamagata-u.ac.jp

J Gastroenterol (2011) 46 (Supplement 1):6–10
DOI 10.1007/s00535-010-0326-1

INTERNATIONAL FORUM

Involvement of activation-induced cytidine deaminase in the development of colitis-associated colorectal cancers

Yoko Endo · Hiroyuki Marusawa · Tsutomu Chiba

Received: 20 April 2010 / Accepted: 6 September 2010 / Published online: 28 September 2010

Abstract Chronic inflammatory bowel disease (IBD) is an important etiologic factor in the development of colorectal cancer. However, the mechanism underlying the development of colorectal cancers through chronic inflammation is not known. Activation-induced cytidine deaminase (AID) was originally identified as an inducer of somatic hypermutation in the immunoglobulin gene. We recently found that the mutagenic activity of AID expression links inflammation to the development of cancer. Aberrant AID expression is triggered by hepatitis C virus infection in human hepatocytes or *Helicobacter pylori* infection in human gastric epithelial cells, and leads to the generation of somatic mutations in various tumor-related genes. Here, we review our findings relating to how AID contributes to the development of colitis-associated colorectal cancers (CACs). Immunohistochemistry revealed the enhanced expression of endogenous AID protein in not only in the inflamed colonic mucosa of ulcerative colitis patients but also CAC tumor lesions. Pro-inflammatory cytokine TNF-α induced strong aberrant expression of AID via IκB kinase-dependent NF-κB-signaling pathways in human colonic epithelial cells. Furthermore, AID expression was also elicited in response to the T helper cell-2-driven cytokines IL-4 and IL-13, which are activated in human IBD. Aberrant activation of AID in colonic cells preferentially evoked genetic mutations in the *TP53* gene, whereas there were no nucleotide alterations of the *APC* gene. These findings suggested that pro-inflammatory cytokine-mediated aberrant expression of AID in colonic epithelial cells plays a role as a genotoxic factor that enhances genetic instability during chronic colonic inflammation, leading to CAC development.

Keywords AID · Inflammatory bowel disease · Colitis-associated colorectal cancer · Cytokine · TP53

Abbreviations

AID	Activation-induced cytidine deaminase
TNF	Tumor necrosis factor
NF-κB	Nuclear factor κB
IKK	IκB kinase
IL	Interleukin

Introduction

Inflammatory bowel disease (IBD) is an important etiologic risk factor for the development of colorectal cancer [1]. The relative risk of colorectal cancer in patients with ulcerative colitis (UC) is 20 times higher than that in the general population [2]. The cumulative risk of colitis-associated colorectal cancer (CAC) increases according to the number of years after disease onset. The cumulative probability of cancer in patients with UC, regardless of the extent of the disease, is 2% at 10 years, 8% at 20 years, and 18% at 30 years [3]. Patients with extensive colitis, colitis lasting 8 years or more, more severe inflammation, and early age onset colitis have the greatest risk of developing cancer [4]. Recently, several studies have shown that not only patients with UC but also those with Crohn's disease (CD) are at risk of developing colon cancer [5]. There is an 18-fold increase in the risk of developing

Y. Endo · H. Marusawa (✉) · T. Chiba
Department of Gastroenterology and Hepatology,
Graduate School of Medicine, Kyoto University,
54 Kawara-cho, Shogoin, Sakyo-ku, Kyoto 606-8507, Japan
e-mail: maru@kuhp.kyoto-u.ac.jp

colorectal cancer in patients with CD compared with the general population [6]. The absolute cumulative risk frequency for developing colorectal cancer is 8% at 22 years from the onset of symptoms in patients with CD. Surveillance colonoscopy is frequently used to detect early cancer lesions in patients with IBD. Surveillance programs are not sufficiently effective to prevent cancers, however, because its diagnosis is difficult. To improve the detection of dysplastic lesions, the mechanisms by which chronic inflammation of the mucosa increases the risk of colorectal cancer development need to be examined.

Nucleotide-editing enzymes that can induce mutations in DNA

Colitis-associated colorectal cancer has several distinct characteristics compared with sporadic colorectal cancers. Adenomatous polyps are the major precursor of sporadic colorectal cancer, and inactivation of the *APC* gene is known to be the initial event in many sporadic colorectal cancers, followed by changes in the *K-ras*, *DCC*, and *TP53* genes [7]. In contrast, mutations in the *TP53* gene are frequently found in early cancer development in UC patients, and are already present in dysplastic lesions [8, 9]. However, the molecular mechanisms underlying the development of the *TP3* mutations in chronic inflamed mucosa that lead to carcinogenesis are not known.

We recently demonstrated that the expression of activation-induced cytidine deaminase (AID), a DNA/RNA-editing enzyme family member, links inflammation to the development of human gastrointestinal and hepatobiliary cancers [10–12]. AID is a member of the apolipoprotein B mRNA-editing catalytic subunit (APOBEC) family; it deaminates cytidine (C) on the target DNA to produce a thymidine (T), leading to the generation of changes in human genome DNA sequences [13]. Under physiologic conditions, AID can induce somatic hypermutation of immunoglobulin genes in activated B cells, which are essential for the diversification of antibody production. However, the fact that high AID expression levels are frequently observed in human lymphoid malignancies suggests that inappropriate AID expression contributes to tumorigenesis due to its mutagenic activity [14]. Consistent with this hypothesis, a transgenic mouse model with constitutive and ubiquitous AID expression develops various tumors through the accumulation of somatic mutations in tumor-related genes [15, 16]. These findings suggest that aberrant AID expression acts as a genome mutator in non-lymphoid tissues and contributes to the development of cancer.

To clarify the role of AID in the development of gastrointestinal cancer, we first determined if there is a link between the regulation of AID expression in hepatocytes and the development of liver cancer [11]. Under physiologic conditions, AID expression is restricted to activated B cells, but we observed aberrant expression of AID in liver tissues exposed to chronic inflammation. Immunohistochemistry and real-time polymerase chain reaction (PCR) showed that AID expression is not normally detected in hepatocytes of noninflamed liver, but endogenous AID expression is significantly elevated in liver tissues with chronic hepatitis and liver cirrhosis. Moreover, aberrant AID expression is induced in response to pro-inflammatory cytokine stimulation or hepatitis C virus infection via the nuclear factor (NF)-κB signaling pathway in human hepatocytes [12]. Similarly, aberrant expression of AID is triggered by *Helicobacter pylori* infection or pro-inflammatory cytokine stimulation in human gastric epithelial cells [10, 17]. We also found that endogenous expression of AID is elevated in bile ducts of primary sclerosing cholangitis, a representative chronic inflammatory disease in bile ducts, and AID expression is also induced after treatment with pro-inflammatory cytokines in human biliary cells [18]. These findings indicate that aberrant AID expression could be commonly induced in response to inflammatory stimulation in gastrointestinal epithelial cells.

Pro-inflammatory cytokines are involved in the regulation of AID expression in human colonic epithelial cells

To study the expression of AID protein in human colonic tissues, we performed immunohistochemistry in human colonic tissues from UC lesions, colitis-associated neoplasms, and nontumorous regions of patients with sporadic colon cancers. In normal colonic mucosa, no immunostaining for AID was observed. In contrast, in UC tissues, immunoreactivity for AID was detected in colonic epithelial cells as well as in infiltrating lymphocytes around the inflamed colonic mucosa [19]. In the colitis-associated neoplasms, AID protein expression was also observed in neoplastic cells in the tumor lesions. These findings indicated that AID protein is expressed in the colonic epithelial cells that are chronically inflamed and in CAC tumor cells.

To determine whether pro-inflammatory cytokines regulate AID transcription in human colonic epithelial cells, we analyzed the expression level of endogenous AID by quantitative reverse transcription PCR and immunoblotting in cultured human colon cancer cells. We first focused on tumor necrosis factor (TNF)-α, which is constitutively activated in the colonic epithelial cells of patients with UC. Only a small amount of endogenous AID expression was detected in quiescent human colonic epithelial cells, but AID expression was markedly elevated after TNF-α

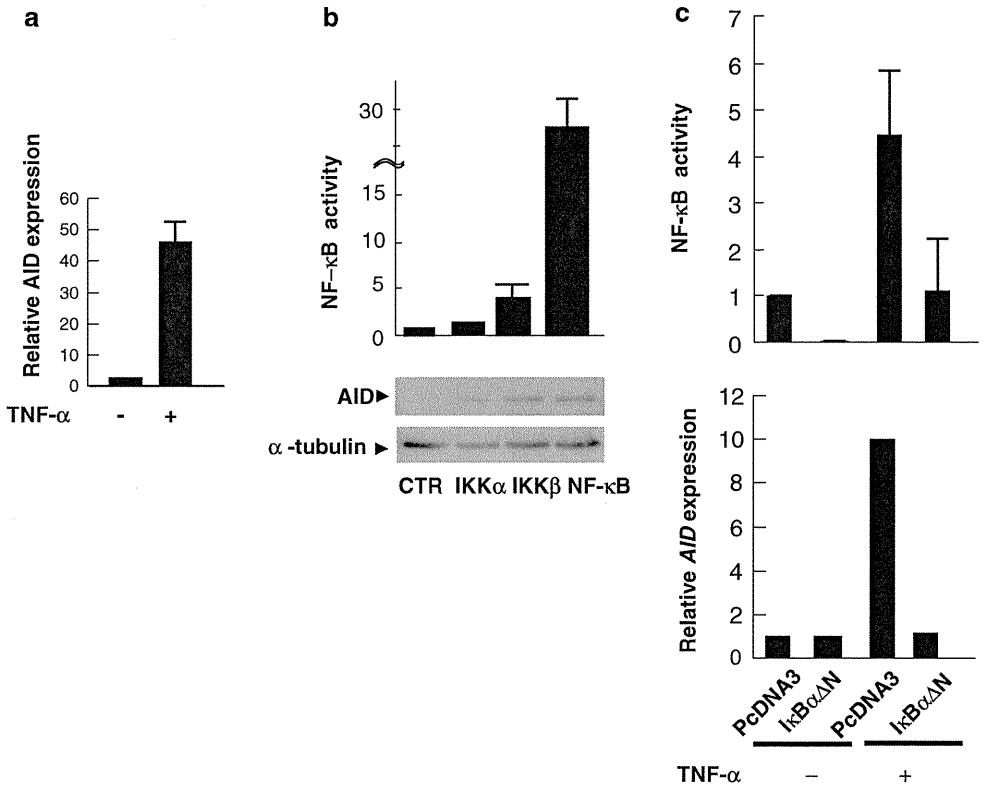

Fig. 1 AID expression is regulated by NF-κB signaling in human colonic epithelial cells. **a** Quantitative PCR for the expression of AID 12 h after stimulation with TNF-α. **b** Immunoblot analysis was performed using anti-human AID antibody from cultured human colonic epithelial cells transfected with expression vector encoding IKKα, IKKβ, NF-κB, or control vector (*lower panel*). **c** Cells were transfected with a vector for the expression of the super-repressor form of IκBα (IκBαΔN) or with a control vector, followed by stimulation with TNF-α for 12 h. Each sample was harvested and luciferase activity was measured to quantify endogenous NF-κB activity (*upper graphs*). Quantitative PCR of AID expression was performed using each specimen as a template (*lower graphs*)

treatment (Fig. 1a). The transcription factor NF-κB is activated by TNF-α signaling. We therefore examined whether AID expression is regulated by the NF-κB signaling pathway in human colon cancer cells. Expression of the positive NF-κB regulators IKKα, IKKβ, and NF-κB itself resulted in the increased expression of endogenous AID protein (Fig. 1b). A negative regulator of NF-κB, the super-repressor form of IκBα, reduced TNF-α mediated AID expression (Fig. 1c). These findings support the idea that AID expression in colonic epithelial cells is regulated through the IKK-dependent NF-κB signaling pathway.

T helper cell (Th) 2 cytokines also play an important role in the pathogenesis of UC. IL-4 and IL-13, which are involved in the Th2 cytokine response, share a common receptor unit and activate transcription factor STAT6 by phosphorylation to induce downstream signal transduction [20]. AID is regulated by the IL-4/STAT6 signaling pathway in B lymphocytes [21]. This finding led us to test whether Th2 cytokines are also involved in the regulation of AID expression in colonic cells. Immunoblotting analysis revealed that IL-4 and IL-13 stimulation induced aberrant AID expression in cultured human colonic epithelial cells (Fig. 2a, b). Further, small interfering RNA specific for STAT6 suppressed IL-13-mediated AID expression (Fig. 2b). These findings suggest that AID expression is regulated by IL-4 and IL-13 in a STAT6-dependent manner in human colonic epithelial cells.

On the other hand, Th1 cytokines are activated dominantly in the colonic epithelial mucosa of patients with CD, and CD patients are also at a high risk for developing colorectal cancer [5]. Interestingly, AID expression is upregulated in cultured colonic cells after treatment with the Th1 cytokine IL-12 (Fig. 2c). Thus, Th1 cytokines may also be involved in aberrant AID expression in human colonic epithelial cells.

AID expression in colonic epithelial cells results in an accumulation of TP53 mutations

The finding that AID expression is induced in colonic cells with chronic inflammation prompted us to examine whether aberrant AID expression could lead to the generation of somatic mutations in tumor-related genes in human colonic epithelial cells. We established a cultured human colonic cell line with constitutive AID expression using a retroviral system, and investigated the mutation frequencies in the *TP53*, *APC*, and *K-ras* genes of colonic epithelial cells in which AID was overexpressed for 8 weeks. No change or only a single nucleotide alteration was detected in all genes from cells transfected with control vectors. In contrast, however, several nucleotide alterations appeared in the *TP53* gene after AID activation [19] (Fig. 3a). Mutation frequencies in the *TP53* gene indicated

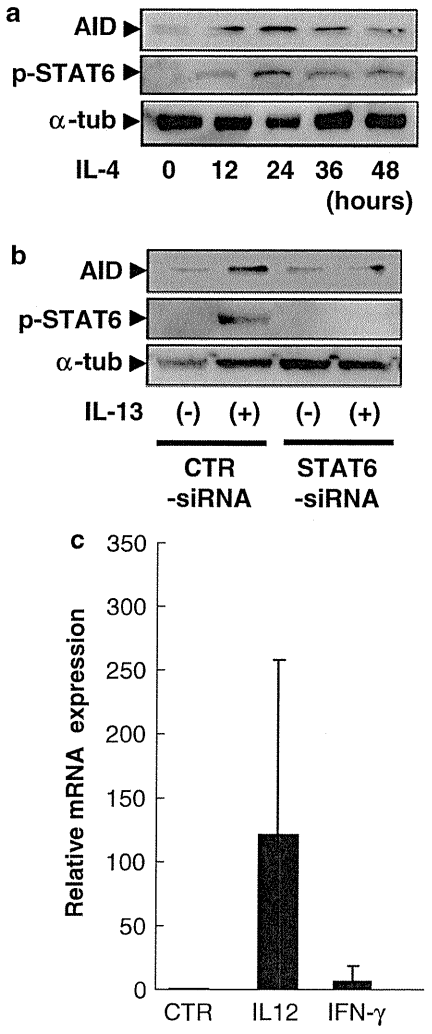

Fig. 2 Regulation of AID expression by Th2 and Th1 cytokine stimulation in human colonic cells. **a** Cells were treated with IL-4 for the indicated times. Total lysates were subjected to immunoblotting using anti-AID (*upper panel*), anti-phosphorylated STAT6 (*middle panel*), or anti-α-tubulin (*lower panel*). **b** Immunoblot analysis was performed using anti-human AID antibody after IL-13 treatment with or without STAT6 small interfering RNA. **c** Quantitative PCR analyses for AID expression in cells treated with IL-12 and interferon-γ

that AID expression increased the mutations in a time-dependent manner (Fig. 3b). In contrast to the *TP53* gene, no nucleotide alterations were detected in the *APC* and *K-ras* genes, even after 8 weeks of AID activation. These findings indicate that aberrant AID expression in human colonic epithelial cells preferentially targets the *TP53* gene, and longer AID activation might induce more mutations. Why the *TP53* gene is more sensitive to AID in human colonic epithelial cells remains unknown. Further studies are required to identify the specific target genes of AID in human colonic epithelial cells. Those genes may become new markers for predicting the development of CAC lesions.

a

Target Genes	Mutation number (n / total bases)	Mutation Frequencies (/10000bp)
TP53	7 / 26400	2.27
APC	0 / 23425	0
K-ras	0 /18760	0

b

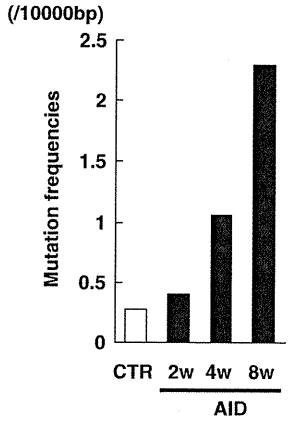

Fig. 3 Mutation frequencies in various tumor-related genes in cultured human colonic epithelial cells with AID activation. **a** Each tumor-related gene was amplified by reverse transcription PCR from cells with 8 weeks of AID activation, the PCR products were subcloned, and sequence analyses were performed. Mutation frequencies were calculated per total bases. **b** Mutation frequencies in the *TP53* gene from cells at 2, 4, and 8 weeks after AID expression, as compared with control cells

Conclusion

The findings of the present study showed that pro-inflammatory cytokines, which play important roles in the pathophysiology of IBD, result in the aberrant expression of AID in human colonic epithelial cells, and lead to the generation of somatic mutations in the *TP53* gene. This is new evidence that might link chronic inflammation of the colonic mucosa to the accumulation of *TP53* mutations, leading to the development of colorectal cancer. It is worth noting that inflammatory-associated AID expression is not limited to colonic epithelial cells. For example, AID expression is induced in response to TNF-α stimulation or hepatitis C virus infection in human hepatocytes via the NF-κB signaling pathway, leading to the accumulation of somatic mutations in various tumor-related genes, including *TP53*. Thus, these findings strongly suggest that aberrant AID expression in various epithelial cells may provide a common link between inflammation, mutational accumulation and cancer development.

Conflict of interest No conflicts of interest exist.

References

1. Podolsky DK. Inflammatory bowel disease. N Engl J Med. 2002;347:417–29.
2. Mellemkjaer L, Olsen JH, Frisch M, Johansen C, Gridley G, McLaughlin JK. Cancer in patients with ulcerative colitis. Int J Cancer. 1995;60:330–3.
3. Eaden JA, Abrams KR, Mayberry JF. The risk of colorectal cancer in ulcerative colitis: a meta-analysis. Gut. 2001;48: 526–35.
4. Lennard-Jones JE, Morson BC, Ritchie JK, Williams CB. Cancer surveillance in ulcerative colitis. Experience over 15 years. Lancet. 1983;2:149–52.
5. Jess T, Gamborg M, Matzen P, Munkholm P, Sorensen TI. Increased risk of intestinal cancer in Crohn's disease: a meta-analysis of population-based cohort studies. Am J Gastroenterol. 2005;100:2724–9.
6. Gillen CD, Walmsley RS, Prior P, Andrews HA, Allan RN. Ulcerative colitis and Crohn's disease: a comparison of the colorectal cancer risk in extensive colitis. Gut. 1994;35:1590–2.
7. Fearon ER, Vogelstein B. A genetic model for colorectal tumorigenesis. Cell. 1990;61:759–67.
8. Yin J, Harpaz N, Tong Y, Huang Y, Laurin J, Greenwald BD, et al. p53 point mutations in dysplastic and cancerous ulcerative colitis lesions. Gastroenterology. 1993;104:1633–9.
9. Kern SE, Redston M, Seymour AB, Caldas C, Powell SM, Kornacki S, et al. Molecular genetic profiles of colitis-associated neoplasms. Gastroenterology. 1994;107:420–8.
10. Matsumoto Y, Marusawa H, Kinoshita K, Endo Y, Kou T, Morisawa T, et al. *Helicobacter pylori* infection triggers aberrant expression of activation-induced cytidine deaminase in gastric epithelium. Nat Med. 2007;13:470–6.
11. Kou T, Marusawa H, Kinoshita K, Endo Y, Okazaki IM, Ueda Y, et al. Expression of activation-induced cytidine deaminase in human hepatocytes during hepatocarcinogenesis. Int J Cancer. 2007;120:469–76.
12. Endo Y, Marusawa H, Kinoshita K, Morisawa T, Sakurai T, Okazaki IM, et al. Expression of activation-induced cytidine deaminase in human hepatocytes via NF-kappaB signaling. Oncogene. 2007;26:5587–95.
13. Muramatsu M, Kinoshita K, Fagarasan S, Yamada S, Shinkai Y, Honjo T. Class switch recombination and hypermutation require activation-induced cytidine deaminase (AID), a potential RNA editing enzyme. Cell. 2000;102:553–63.
14. Kinoshita K, Nonaka T. The dark side of activation-induced cytidine deaminase: relationship with leukemia and beyond. Int J Hematol. 2006;83:201–7.
15. Okazaki IM, Hiai H, Kakazu N, Yamada S, Muramatsu M, Kinoshita K, et al. Constitutive expression of AID leads to tumorigenesis. J Exp Med. 2003;197:1173–81.
16. Morisawa T, Marusawa H, Ueda Y, Iwai A, Okazaki IM, Honjo T, et al. Organ-specific profiles of genetic changes in cancers caused by activation-induced cytidine deaminase expression. Int J Cancer. 2008;123:2735–40.
17. Chiba T, Marusawa H, Seno H, Watanabe N. Mechanism for gastric cancer development by *Helicobacter pylori* infection. J Gastroenterol Hepatol. 2008;23:1175–81.
18. Komori J, Marusawa H, Machimoto T, Endo Y, Kinoshita K, Kou T, et al. Activation-induced cytidine deaminase links bile duct inflammation to human cholangiocarcinoma. Hepatology. 2008; 47:888–96.
19. Endo Y, Marusawa H, Kou T, Nakase H, Fujii S, Fujimori T, et al. Activation-induced cytidine deaminase links between inflammation and the development of colitis-associated colorectal cancers. Gastroenterology 2008;135:889–98, 898 e1–3.
20. Hebenstreit D, Wirnsberger G, Horejs-Hoeck J, Duschl A. Signaling mechanisms, interaction partners, and target genes of STAT6. Cytokine Growth Factor Rev. 2006;17:173–88.
21. Dedeoglu F, Horwitz B, Chaudhuri J, Alt FW, Geha RS. Induction of activation-induced cytidine deaminase gene expression by IL-4 and CD40 ligation is dependent on STAT6 and NFkappaB. Int Immunol. 2004;16:395–404.

Genetic Heterogeneity of Hepatitis C Virus in Association with Antiviral Therapy Determined by Ultra-Deep Sequencing

Akihiro Nasu[1], Hiroyuki Marusawa[1]*, Yoshihide Ueda[1], Norihiro Nishijima[1], Ken Takahashi[1], Yukio Osaki[2], Yukitaka Yamashita[3], Tetsuro Inokuma[4], Takashi Tamada[5], Takeshi Fujiwara[6], Fumiaki Sato[6], Kazuharu Shimizu[6], Tsutomu Chiba[1]

1 Department of Gastroenterology and Hepatology, Graduate School of Medicine, Kyoto University, Kyoto, Japan, **2** Department of Gastroenterology and Hepatology, Osaka Red Cross Hospital, Osaka, Japan, **3** Department of Gastroenterology and Hepatology, Wakayama Red Cross Hospital, Wakayama, Japan, **4** Department of Gastroenterology, Kobe City Medical Center General Hospital, Kobe, Japan, **5** Department of Gastroenterology and Hepatology Takatsuki Red Cross Hospital, Osaka, Japan, **6** Department of Nanobio Drug Discovery, Graduate School of Pharmaceutical Sciences, Kyoto University, Kyoto, Japan

Abstract

Background and Aims: The hepatitis C virus (HCV) invariably shows wide heterogeneity in infected patients, referred to as a quasispecies population. Massive amounts of genetic information due to the abundance of HCV variants could be an obstacle to evaluate the viral genetic heterogeneity in detail.

Methods: Using a newly developed massive-parallel ultra-deep sequencing technique, we investigated the viral genetic heterogeneity in 27 chronic hepatitis C patients receiving peg-interferon (IFN) α2b plus ribavirin therapy.

Results: Ultra-deep sequencing determined a total of more than 10 million nucleotides of the HCV genome, corresponding to a mean of more than 1000 clones in each specimen, and unveiled extremely high genetic heterogeneity in the genotype 1b HCV population. There was no significant difference in the level of viral complexity between immediate virologic responders and non-responders at baseline ($p = 0.39$). Immediate virologic responders ($n = 8$) showed a significant reduction in the genetic complexity spanning all the viral genetic regions at the early phase of IFN administration ($p = 0.037$). In contrast, non-virologic responders ($n = 8$) showed no significant changes in the level of viral quasispecies ($p = 0.12$), indicating that very few viral clones are sensitive to IFN treatment. We also demonstrated that clones resistant to direct-acting antivirals for HCV, such as viral protease and polymerase inhibitors, preexist with various abundances in all 27 treatment-naïve patients, suggesting the risk of the development of drug resistance against these agents.

Conclusion: Use of the ultra-deep sequencing technology revealed massive genetic heterogeneity of HCV, which has important implications regarding the treatment response and outcome of antiviral therapy.

Citation: Nasu A, Marusawa H, Ueda Y, Nishijima N, Takahashi K, et al. (2011) Genetic Heterogeneity of Hepatitis C Virus in Association with Antiviral Therapy Determined by Ultra-Deep Sequencing. PLoS ONE 6(9): e24907. doi:10.1371/journal.pone.0024907

Editor: Yoshio Yamaoka, Veterans Affairs Medical Center (111D), United States of America

Received June 17, 2011; **Accepted** August 19, 2011; **Published** September 22, 2011

Funding: This study was supported by Japan Society for the Promotion of Science (JSPS) Grants-in-aid for Scientific Research, and Health and Labour Sciences Research Grants for Research, and Research on Hepatitis from the Ministry of Health, Labour and Welfare, Japan. The funders had no role in study design, data collection and analysis, decision to publish, or preparation of the manuscript.

Competing Interests: The authors have declared that no competing interests exist.

* E-mail: maru@kuhp.kyoto-u.ac.jp

Introduction

Hepatitis C virus (HCV) is classified as a member of the Flaviviridae family [1] and has an approximately 9.6-kb single-stranded RNA genome. This RNA genome encodes a large precursor polyprotein, which is cleaved by viral and host proteases to generate at least 10 functional viral proteins; core, envelope (E)-1, E2, p7, nonstructural protein (NS)-2, NS3, NS4A, NS4B, NS5A, and NS5B [2,3]. A strong characteristic of HCV infection is its significant genetic diversity, the consequence of the absence of proofreading activity in RNA-dependent RNA polymerase [4], and the high level of viral replication during its life cycle [5]. The mean frequency of nucleotide alterations occurring in HCV RNA is calculated to be between 1.4×10^3 and 1.9×10^3 substitutions per nucleotide per year [6,7]. As a result, the infecting HCV clones in each patient invariably show population diversity with a high degree of genetic heterogeneity. The collection of viruses in a population of closely related but non-identical genomes is referred to as a quasispecies [8,9], and the dominant viral population may be evolving as a result of its viral replicative fitness and concurrent immune selection pressures that drive clonal selection.

It is reasonable to assume that the viral pathogenesis and sensitivity to treatment are affected by the generation of escape mutants through immune evasion and the modification of virulence characteristics by anti-viral treatment [10]. Thus, certain viral mutations have important implications for the pathogenesis of the viral disease and the sensitivity to antiviral therapy. Several studies have attempted to associate genetic heterogeneity or

number of mutations with pathogenesis and treatment outcome. However, the abundant diversity and complexity of the chronically-infected HCV has been an obstacle to evaluate the viral genetic heterogeneity in detail. In this respect, the recent introduction of ultra-deep sequencing technology, capable of producing millions of DNA sequence reads in a single run, is rapidly changing the landscape of genome research [11,12]. One application of ultra-deep sequencing was the identification of rare minority drug resistant clones of human immunodeficiency virus, which are not detectable by standard sequencing techniques [13–15]. Moreover, the recent study using 454/Roche pyrosequencing technology clarified the transmission bottlenecks by measuring the population structure within patients with HCV infection [16].

In this study, we used for the first time ultra-deep sequencing with Illumina Genome Analyzer II (Illumina, San Diego, CA) and determined the pictures of viral quasispecies of genotype 1b HCV in patients receiving peg-interferon (IFN) α2b plus ribavirin (RBV) to clarify the significance of the viral genetic complexity in the pathophysiology of HCV infection and the treatment outcome of the current IFN-based therapy for HCV-infected patients. Because our main objective was to determine whether the HCV sequence variation itself is responsible for the sensitivity or resistance to antiviral therapy, we compared the composition of the HCV population complexity 1 week after IFN administration in patients who showed a prompt decrease in HCV viremia with those in whom there was no reduction in the serum HCV RNA levels after the initiation of IFN treatment. We also examined the prevalence of drug-resistant mutations to direct-acting antivirals (DAAs) for HCV in treatment-naïve HCV-infected patients, based on the fact that drug-resistant mutations already exist in treatment-naïve patients with various pathogenic virus infections, such as human immunodeficiency viruses [14,17].

Results

Validation of multiplex ultra-deep sequencing of the HCV genome

We performed a massive parallel ultra-deep sequencing run on the Illumina Genome Analyzer II platform using multiplex tagging methods. First, we conducted a control experiment to validate the efficacy and error rates in ultra-deep sequencing of the viral genome. For this purpose, we used a plasmid encoding full-length HCV [18] as a template and determined the plasmid-derived whole HCV sequence. The ultra-deep sequencing platform provided us the full-length HCV genome information derived from the plasmids with a mean coverage of 1674.3 at each nucleotide site (Table 1). Errors comprised insertions (1.0%), deletions (4.2%), and nucleotide mismatches (94.8%) and the overall error rates by multiplex ultra-deep sequencing were determined to be a mean of 0.0010 per bp. Next we confirmed that the high-fidelity PCR amplification with HCV-specific primer sets followed by multiplex ultra-deep sequencing resulted in no significant increase in the error rates in the viral sequencing data (ranging from 0.0012 to 0.0013 per bp; per-nucleotide error rate, 0.12%–0.13%).

To estimate the accuracy of detecting nucleotide alterations using reads filtered by average base quality and mapping quality, we introduced the plasmid with single point mutations within the wild-type viral sequences with the ratio of 1:99 and 1:999 and assessed the sensitivity and accuracy of quantification with the high-fidelity PCR amplification followed by multiplex ultra-deep sequencing. Duplicate control experiments revealed that mutations present at an input ratio of 0.10% ranged between 0.09 and 0.19%, and the results could be reproducibly quantified (data not shown). Based on these results, we picked up the low abundant mutations that presented at frequency of more than 0.20% among the total viral clones, a level that could rule out putative errors caused by massively-parallel sequencing, in the current platform used in this study.

Table 1. Error frequency of ultra-deep sequencing for the plasmid encoding full-genome HCV sequence.

	PCR amplification	
	(−)*	(+)*
Total read nucleotides	15,118,929	24,158,372
Mean coverage	1674.3	5562.6
Type of errors		
mismatches	14,629 (94.8%)	26,243 (88.6%)
deletions	640 (4.2%)	2510 (8.5%)
insertions	147 (1.0%)	859 (2.9%)
Overall error rate (%)	0.102	0.123

*(−); Ultra-deep sequencing of HCV encoding plasmid
(+); Ultra-deep sequencing of PCR-amplified HCV encoding plasmid.
doi:10.1371/journal.pone.0024907.t001

Large heterogeneity of viral clones in HCV-infected patients

HCV infection comprises a heterogeneous mixture of viral clones with various mutations. To clarify the landscape of HCV heterogeneity as a quasispecies, we determined the viral full-genome sequences derived from 27 HCV-infected patients by multiplex ultra-deep sequencing and compared the results with those obtained by the direct population Sanger sequencing method. All sequence reads by multiplex ultra-deep sequencing have been deposit in DNA Data Bank of Japan Sequence Read Archive (http://www.ddbj.nig.ac.jp/index-e.html) under accession number DRA000366.

HCV nucleotide sequence reads by ultra-deep sequencing were aligned to the consensus viral sequences in the same serum specimen that were determined by direct population Sanger sequencing. A mean number of 1705-fold coverage on average was achieved at each nucleotide site of the HCV sequences in each specimen. The average frequencies of altered sequences detected in each viral genomic region are summarized in Table 2. Compared with the representative sequence of the population average clone, the mutation frequency was 1.04% of the total viral genomic sequences and 16.1% of the total nucleotide positions on average. Most of the genomic changes observed in viral variants were single base substitutions and unevenly distributed throughout the region of the HCV genome.

Among the viral genomic regions, the nucleotide sequence complexity expressed as the Shannon entropy was smallest in the core region. In contrast, the viral sequence complexity in the E2 region was highest among the HCV genomic regions and significantly greater than the average mutation frequency of the remaining HCV genome ($p = 0.0026$). Similarly, the ratio of the number of mutated nucleotides to the total number of nucleotides analyzed in the E2 region was significantly higher than that of the remaining HCV genome ($p = 5.66 \times 10^{-6}$). These findings clearly confirmed that the quasispecies complexity in E2, which contains hypervariable region1 (HVR1) and HVR2, was prominently larger than that of other viral genomic regions [19].

Table 2. Mean genetic complexity of the genotype1b HCV in chronically infected 27 patients.

Viral genomic Region	Mean number of aligned nucleotides	Mean number of mutated nucleotides	Mean coverage	Mutation frequency (%)	Mean Shannon entropy
Core	779,839	5027	1361	0.61	0.045926
E1	739,220	7902	1360	0.99	0.064884
E2	1,382,907	19,724	1265	1.37	0.088584
p7	217,000	3237	1148	1.44	0.075829
NS2	673,579	8702	1073	1.19	0.075333
NS3	4,958,188	52,204	2619	0.93	0.060767
NS4A	427,677	5604	2640	1.32	0.072217
NS4B	1,209,000	17,485	1544	1.26	0.063190
NS5A	2,034,626	28,820	1518	1.28	0.067398
NS5B	2,720,417	27,449	1681	0.90	0.054805
Total	14,875,801	172,327	1705	1.04	0.062624

doi:10.1371/journal.pone.0024907.t002

Early dynamic changes of viral complexity after the administration of peg-IFNα2b plus RBV

Among 27 patients enrolled in this study, 8 showed a prompt decrease in their serum HCV RNA levels and 8 showed no significant changes 1 week after initiating treatment with peg-IFNα2b plus RBV. To clarify the changes in the viral quasispecies in response to antiviral therapy, we determined the early dynamic changes in viral complexity before and after 1 week of peg-IFNα2b plus RBV administration in these 8 immediate virologic responders and 8 non-responders. All cases were infected with genotype 1b viruses, and the clinical features, including serum HCV RNA level at baseline, did not significantly differ between immediate virologic responders and non-responders (Table 3). A mean coverage of 1798-fold and 2416-fold were mapped to each reference sequence in immediate virologic responders before and after peg-IFNα2b plus RBV administration, respectively. Similarly, a mean coverage of 1780-fold and 2461-fold were determined in non-responders before and after peg-IFNα2b plus RBV administration, respectively (Table 4 and Table S1).

We then estimated the genomic complexity by calculating the Shannon entropy for each nucleotide position before and after the administration of peg-IFNα2b plus RBV (Table 4). There was no significant difference in the level of viral complexity between immediate virologic responders and non-responders at a baseline (mean Shannon entropy value 0.072 vs 0.075, $p = 0.39$). Immediate virologic responders, however, showed a significant reduction in the nucleotide sequence complexity after the administration of peg-IFNα2b plus RBV (mean Shannon entropy value 0.072 vs 0.049, $p = 0.037$), indicating that the viral quasispecies nature after the peg-IFNα2b plus RBV treatment

Table 3. Characteristics of patients that showed immediate virologic response or non-response to PEG-IFNα2b plus ribavirin combination therapy.

	Immediate virologic responders	Non-responders	P-value
Age†	50.5 (45–68)	60 (55–69)	0.12
Sex (male/female)	5/3	5/3	1
Alanine aminotransaminase† (IU/l)	54 (15–198)	72 (30–143)	0.51
Total bilirubin† (mg/dl)	0.6 (0.4–1.8)	0.8 (0.4–1.4)	0.34
Platelet count† ($\times 10^4/mm^3$)	18.9 (7.1–27.2)	16.7 (11.6–22.5)	0.68
HCV genotype	1b	1b	
HCV viral load† (log IU/ml)			
pre-treatment	6.6 (6.2–7.5)	6.9 (6.1–7.6)	0.43
after treatment	4.6 (4.0–5.2)	6.5 (6.1–6.8)	**0.028**
Final outcome			**0.025**
sustained viral response	6	0	
Relapse	1	1	
non-response	0	6	
withdraw*	1	1	

† Values are median (range).
* The treatment was discontinued in one immediate virologic responder and one non-responder, due to the side effect of IFN and the development of liver cancer, respectively.
doi:10.1371/journal.pone.0024907.t003

Table 4. Genetic complexity at pre-treatment and 1 week after PEG-IFNα2b plus ribavirin combination therapy in immediate virologic responders and non-responders.

	Immediate virologic responders (N = 8)		Non-responders (N = 8)	
	Pre-treatment	**1 week after IFN therapy**	**Pre-treatment**	**1 week after IFN therapy**
Mean number of aligned reads	263,452	356,963	256615	354,398
Mean number of aligned nucleotides	16,632,186	22,438,125	16,248,820	22,379,922
Mean coverage	1798	2416	1780	2461
Mutation frequency (%)	0.96	0.63	1.13	1.11
Shannon entropy	0.072*	0.049*	0.075**	0.066**

Wilcoxon rank sum test.
* $p = 0.037$.
** $p = 0.12$.
doi:10.1371/journal.pone.0024907.t004

became relatively more homogeneous than at baseline status in this group. In contrast, no significant changes in the nucleotide sequence complexity were observed in non-responder patients before and after treatment with peg-IFNα2b plus RBV (mean Shannon entropy value 0.075 vs 0.066, $p = 0.12$). We then examined whether specific nucleotide position might be associated with the response to peg-IFNα2b plus RBV treatment in immediate virologic responders, but complexity was not commonly shared at any specific nucleotide position that changed by more than 50% after peg-IFNα2b plus RBV administration (data not shown), indicating no association between the specific nucleotide position and the response to peg-IFNα2b plus RBV treatment.

Elimination of minor viral clones by peg-IFNα2b plus RBV therapy

Next, we compared the nucleotide complexity in each viral genomic region of the immediate virologic responders with that of non-responders before and after peg-IFNα2b plus RBV administration (Figure 1 and Table S2). In immediate virologic responders, the peg-IFNα2b plus RBV therapy induced a significant reduction in the nucleotide sequence complexity in all viral genomic regions except NS4B. In contrast, non-responders showed no significant change in the viral sequence complexity in any viral genomic region. For example, there was no significant difference in the mean complexity in the E2 region at baseline between the immediate virologic responders and non-responders. The administration of peg-IFNα2b plus RBV significantly reduced the levels of nucleotide sequence complexity in the E2 region in all the immediate virologic responders (mean Shannon entropy value 0.139 vs 0.085, respectively. $p = 0.012$, Figure 1 and Table S2). In contrast, no significant changes in the sequence complexity were observed in the E2 (mean Shannon entropy value 0.083 vs 0.082, respectively. $p = 0.89$) regions in non-responder cases after treatment with peg-IFNα2b plus RBV.

To examine whether certain viral clones in non-responders showed sensitivity to IFN therapy, we investigated the sequence complexity in HVR1 in the E2 region in detail before and after peg-IFNα2b plus RBV therapy, because the HVR1 region possessed one of the highest complexities among viral genomic regions. In immediate virologic responders, the heterogeneity at each nucleotide position was reduced in response to peg-IFNα2b plus RBV administration (representative nucleotide changes are shown in Figure 2A). In contrast, the ratio of mutated clones among the total sequence reads determined at each nucleotide site in HVR1 showed no significant change before and after the administration of peg-IFNα2b plus RBV in the majority of non-responders (Figure 2B), suggesting that very few viral clones showed sensitivity to peg-IFNα2b plus RBV and were eliminated after the administration of peg-IFNα2b plus RBV.

Detection of viral clones with drug-resistant mutations

Because none of the DAAs for HCV were approved by Japanese health coverage at the time of this study, all patients enrolled into this study were naïve to DAAs for HCV including protease and polymerase inhibitors. Thus, we determined whether the reported drug-resistant mutants exist spontaneously in nature among treatment-naïve HCV-infected patients. For this purpose, we examined the naturally prevalent mutations against HCV protease and polymerase inhibitors in the 27 patients. The drug-resistant mutations examined here included 9 mutations resistant to NS3/4 protease inhibitors, including Telaprevir, Boceprevir, TMC435350, ITMN191/R7227, MK-7009, and BI-201335, and 5 mutations resistant to NS5B polymerase inhibitors, including Filibuvir, BI-207127, and R7128 [20].

The mean number of sequence reads at the nucleotide position comprising mutations resistant to NS3/4A protease and NS5B polymerase inhibitors among the 27 cases were obtained with 1179-fold and 1972-fold coverage, respectively. Based on the detection rate of the low-level viral clones determined by the control experiments, we picked up the drug-resistant mutants that presented at a frequency of more than 0.2% among the total viral clones. Based on these criteria, at least one resistant mutation was detected in all subjects (Table 5). The mean prevalence of the 14 drug-resistant mutations ranged from 0.20% to 99.1% indicating that the proportion of resistant mutations substantially differed in each case. The T54S/A mutation resistant to Teraprevir and Boceprevir in genotype 1b HCV [21] was the most commonly detected (20 of 27 cases, 74.1%). The proportion of T54S/A mutations among the total clones ranged from 0.21% to 86.9% and thus substantially differed between cases. Other mutations resistant to the NS3/4A protease-inhibitor were detected in 16 of 27 cases (59.3%) at V55A and Q80R/K, and 12 of 27 cases (44.4%) at V36A/M. In contrast, no D168A/V/T/H mutation resistant to ITMN191/R7227, MK-7009, TMC435350, and BI-201335 was detectable. Regarding NS5B polymerase inhibitors, the V499A mutation resistant to BI-207127, was most frequently detected and 20 of 27 (74.1%) of subjects possessed the resistant-mutant clones at levels 0.20% to 99.1% at baseline. Only one case had the BI-207127-resistant P496A mutant clones and none had the R7128-resistant S282T clones. Of the 27 subjects, 16 (59.3%) harbored mutations resistant to at least four kinds of NS5B polymerase inhibitors and/or NS3/4A protease-inhibitors. More-

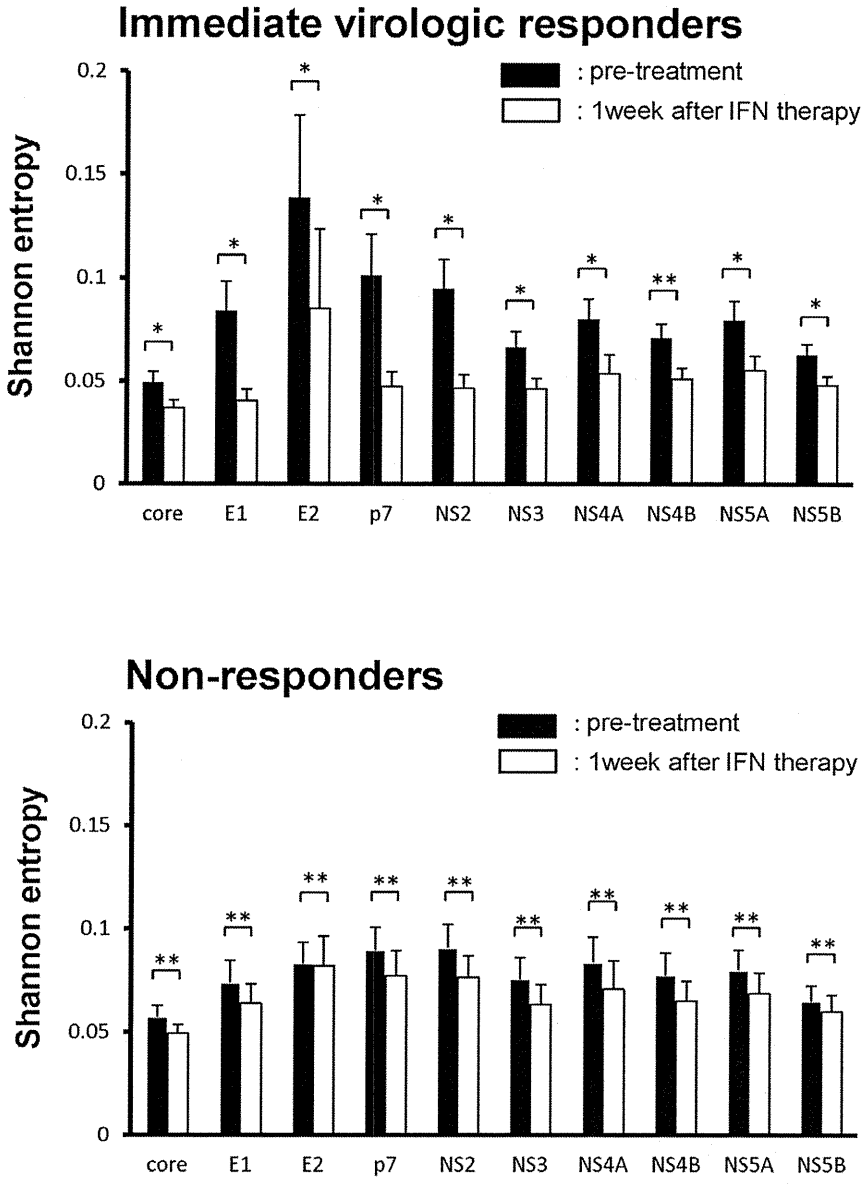

Figure 1. Changes in the genetic complexity of each HCV genomic region before and after the administration of peg-IFNα2b plus RBV. Shannon entropy values at baseline (black bar) and 1 week after initiation of treatment with peg-IFNα2b plus RBV (white bar) in 8 immediate virologic responders (A) and in 8 non-responders (B) are shown. * $p<0.05$, ** not significant. (Mean values ± SD; n = 8)
doi:10.1371/journal.pone.0024907.g001

over, 5 subjects (18.5%) harbored resistance to 6 antiviral drugs. Notably, 3 subjects harbored resistance to 8 of 9 antiviral drugs. There was no significant association between the frequency of drug-resistant mutations and the serum viral load ($r = 0.0678$) (Figure S1).

These findings indicate that drug-resistant HCV variants are present in a considerable proportion among the chronically HCV-infected, DAAs-naïve patients.

Discussion

Sequence heterogeneity, so-called quasispecies, is a common feature of RNA viruses, including HCV [22]. Previous studies of the viral genome with conventional Sanger sequencing methods revealed that HCV infection comprises a cloud of closely related sequence variants differing by as little as one nucleotide from a population average sequence [23]. A number of studies have aimed to clarify the significance of viral mutations in association with clinical features, including viral persistency and chronicity, degree of liver damage, response to treatment, and selection of mutants resistant to anti-viral therapy. The quasispecies nature of HCV, however, represents a major obstacle in determining the significance of the viral clone with specific sequence characteristics. Newly developed ultra-deep sequencing analysis allowed us to clarify the whole picture of viral quasispecies present in chronically HCV-infected patients. In the present study, ultra-deep sequencing determined a mean total of more than 10 million nucleotides of the viral genome in each specimen, representing more than 1000 clones infecting each patient, thus demonstrating the abundant genetic complexity of HCV.

It is well recognized that the HCV genome is heterogeneous at the intra-individual level [9,10]. The current ultra-deep sequenc-

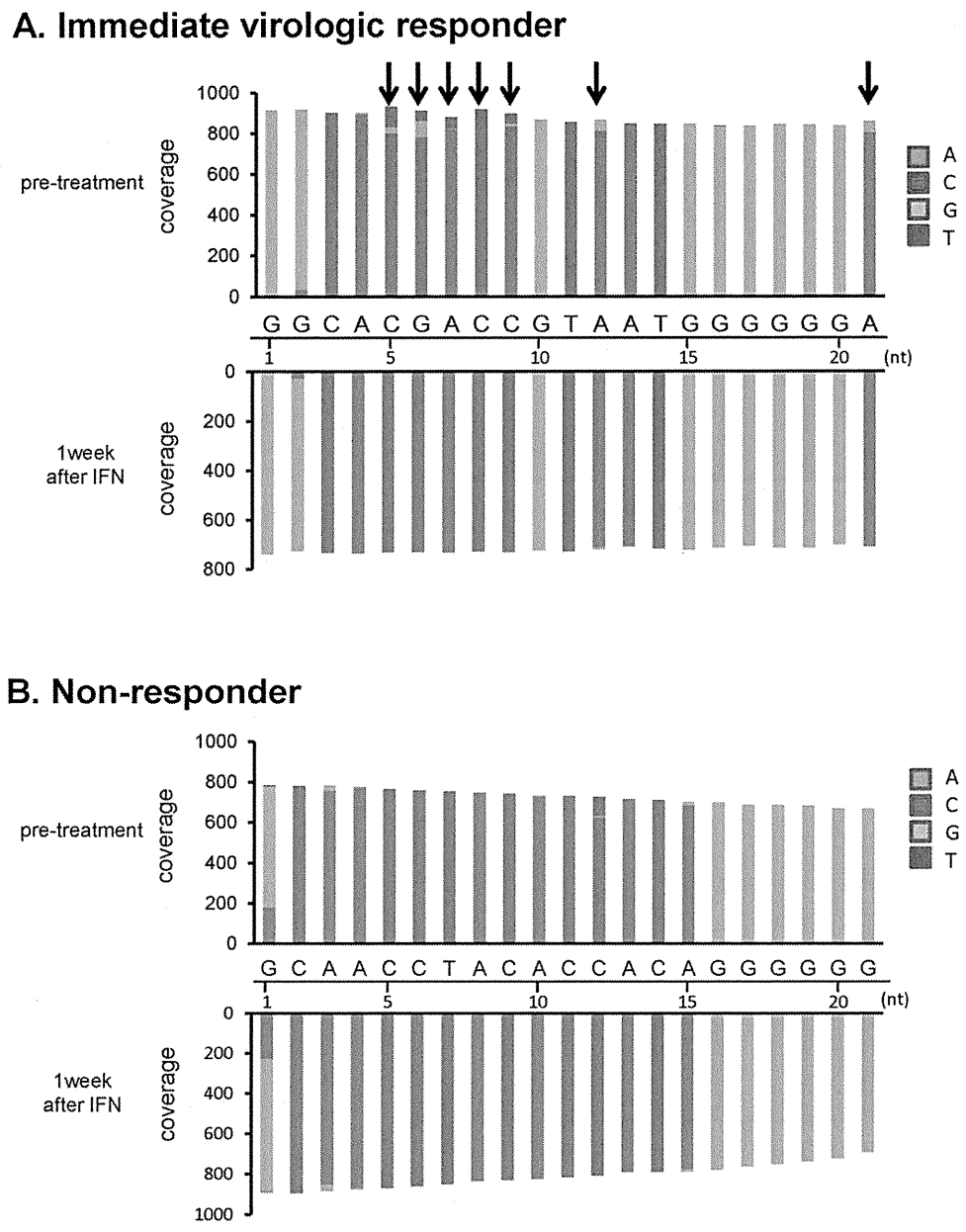

Figure 2. Ratio of mutated nucleotides in the HVR1 region before and after administration of peg-IFNα2b plus RBV therapy. Representative results of a immediate virologic responder (Patient#3) (**A**) and a non-responder (Patient#9) (**B**) are shown. The read numbers (coverage) at each nucleotide position of the HVR1 (from 1st nucleotide to 21st nucleotide in E2 region) at pre-treatment (upper graphs) and 1 week after initiating treatment with peg-IFNα2b plus RBV (lower graphs) are shown. Arrows indicate the nucleotide positions that showed the elimination of minor mutant clones after administration of peg-IFNα2b plus RBV.
doi:10.1371/journal.pone.0024907.g002

ing analyses revealed that the E2 region had the highest sequence heterogeneity, while the core region had the lowest sequence heterogeneity among the viral genomic regions encoding different functional viral proteins. More than 15% of nucleotides in the E2 region were mutated in all cases examined. These findings are consistent with previous conventional Sanger sequencing-based studies showing that HVR1 and HVR2 possess the highest sequence diversity among the HCV genomic regions [19] and that the highest values of mean Shannon entropy at the HCV 1a population level are in the E2 region [24].

Various mutations in the HCV genome are associated with the therapeutic response. For example, a number of mutations within a so-called IFNα sensitivity determining region of NS5A are closely associated with sensitivity to IFN-based anti-viral therapy [25,26]. A recent study also showed that amino acid substitution in the HCV core region could be a useful predictor of the virologic response to peg-IFNα plus RBV combination therapy [27]. Although the findings of these studies suggested that certain mutations in the representative HCV clone could predict treatment outcome, it is unknown whether the specific viral clone comprising those mutations directly displays sensitivity or resistance to anti-viral therapy. In the present study, sequential comparison of the HCV1b genome derived at baseline and at 1 week after the administration of peg-IFNα2b plus RBV demon-